The Astrophysical Journal Letters, 984:L41 (8pp), 2025 May 10 https://doi.org/10.3847/2041-8213/adcc29

On the Potential Cosmogenic Origin of the Ultra-high-energy Event KM3-230213A

O. Adriani[1,2], S. Aiello[3], A. Albert[4,5], A. R. Alhebsi[6], M. Alshamsi[7], S. Alves Garre[8], A. Ambrosone[9,10], F. Ameli[11], M. Andre[12], L. Aphecetche[13], M. Ardid[14], S. Ardid[14], C. Argüelles[15], J. Aublin[16], F. Badaracco[17,18], L. Bailly-Salins[19], Z. Bardačová[20,21], B. Baret[16], A. Bariego-Quintana[8], Y. Becherini[16], M. Bendahman[10], F. Benfenati Gualandi[22,23], M. Benhassi[10,24], M. Bennani[19], D. M. Benoit[25], E. Berbee[26], E. Berti[1], V. Bertin[7], P. Betti[1], S. Biagi[27], M. Boettcher[28], D. Bonanno[27], S. Bottai[1], A. B. Bouasla[29], J. Boumaaza[30], M. Bouta[7], M. Bouwhuis[26], C. Bozza[10,31], R. M. Bozza[9,10], H. Brânzaş[32], F. Bretaudeau[13], M. Breuhaus[7], R. Bruijn[26,33], J. Brunner[7], R. Bruno[3], E. Buis[26,34], R. Buompane[10,24], J. Busto[7], B. Caiffi[17], D. Calvo[8], A. Capone[11,35], F. Carenini[22,23], V. Carretero[26,33], T. Cartraud[16], P. Castaldi[23,36], V. Cecchini[8], S. Celli[11,35], L. Cerisy[7], M. Chabab[37], A. Chen[38], S. Cherubini[27,39], T. Chiarusi[23], M. Circella[40], R. Clark[41], R. Cocimano[27], J. A. B. Coelho[16], A. Coleiro[16], A. Condorelli[16,63], R. Coniglione[27], P. Coyle[7], A. Creusot[16], G. Cuttone[27], R. Dallier[13], A. De Benedittis[10], G. De Wasseige[41], V. Decoene[13], P. Deguire[7], I. Del Rosso[22,23], L. S. Di Mauro[27], I. Di Palma[11,35], A. F. Díaz[42], D. Diego-Tortosa[27], C. Distefano[27], A. Domi[43], C. Donzaud[16], D. Dornic[7], E. Drakopoulou[44], D. Drouhin[4,5], J.-G. Ducoin[7], P. Duverne[16], R. Dvornický[20], T. Eberl[43], E. Eckerová[20,21], A. Eddymaoui[30], T. van Eeden[26], M. Eff[16], D. van Eijk[26], I. El Bojaddaini[45], S. El Hedri[16], S. El Mentawi[7], V. Ellajosyula[17,18], A. Enzenhöfer[7], G. Ferrara[27,39], M. D. Filipović[46], F. Filippini[23], D. Franciotti[27], L. A. Fusco[10,31], T. Gal[43], J. García Méndez[14], A. Garcia Soto[8], C. Gatius Oliver[26], N. Geisselbrecht[43], E. Genton[41], H. Ghaddari[45], L. Gialanella[10,24], B. K. Gibson[25], E. Giorgio[27], I. Goos[16], P. Goswami[16], S. R. Gozzini[8], R. Gracia[43], C. Guidi[17,18], B. Guillon[19], M. Gutiérrez[47], C. Haack[43], H. van Haren[48], A. Heijboer[26], L. Hennig[43], J. J. Hernández-Rey[8], A. Idrissi[27], W. Idrissi Ibnsalih[10], G. Illuminati[23], O. Janik[43], D. Joly[7], M. de Jong[26,49], P. de Jong[26,33], B. J. Jung[26], P. Kalaczyński[50,51], N. Kamp[15], J. Keegans[25], V. Kikvadze[52], G. Kistauri[52,53], C. Kopper[43], A. Kouchner[16,54], Y. Y. Kovalev[55], L. Krupa[21], V. Kueviakoe[26], V. Kulikovskiy[17], R. Kvatadze[53], M. Labalme[19], R. Lahmann[43], M. Lamoureux[41], G. Larosa[27], C. Lastoria[19], J. Lazar[41], A. Lazo[8], S. Le Stum[7], G. Lehaut[19], V. Lemaître[41], E. Leonora[3], N. Lessing[8], G. Levi[22,23], M. Lindsey Clark[16], F. Longhitano[3], F. Magnani[7], J. Majumdar[26], L. Malerba[17,18], F. Mamedov[21], A. Manfreda[10], A. Manousakis[56], M. Marconi[17,18], A. Margiotta[22,23], A. Marinelli[9,10,63], C. Markou[44], L. Martin[13], M. Mastrodicasa[11,35], S. Mastroianni[10], J. Mauro[41], K. C. K. Mehta[51], A. Meskar[57], G. Miele[9,10], P. Migliozzi[10], E. Migneco[27], M. L. Mitsou[10,24], C. M. Mollo[10], L. Morales-Gallegos[10,24], N. Mori[1], A. Moussa[45], I. Mozun Mateo[19], R. Muller[23], M. R. Musone[10,24], M. Musumeci[27], S. Navas[47], A. Nayerhoda[40], C. A. Nicolau[11], B. Nkosi[38], B. Ó Fearraigh[17], V. Oliviero[9,10], A. Orlando[27], E. Oukacha[16], L. Pacini[1], D. Paesani[27], J. Palacios González[8], G. Papalashvili[40,52], P. Papini[1], V. Parisi[17,18], A. Parmar[19], E.J. Pastor Gomez[8], C. Pastore[40], A. M. Păun[32], G. E. Păvălaş[32], S. Peña Martínez[16], M. Perrin-Terrin[7], V. Pestel[19], R. Pestes[16], M. Petropavlova[21,58], P. Piattelli[27], A. Plavin[55,59], C. Poirè[10,31], V. Popa[32,64], T. Pradier[4], J. Prado[8], S. Pulvirenti[27], C.A. Quiroz-Rangel[14], N. Randazzo[3], A. Ratnani[60], S. Razzaque[61], I. C. Rea[10], D. Real[8], G. Riccobene[27], J. Robinson[28], A. Romanov[17,18,19], E. Ros[55], A. Šaina[8], F. Salesa Greus[8], D. F. E. Samtleben[26,49], A. Sánchez Losa[8], S. Sanfilippo[27], M. Sanguineti[17,18], D. Santonocito[27], P. Sapienza[27], M. Scaringella[1], M. Scarnera[16,41], J. Schnabel[43], J. Schumann[43], H. M. Schutte[28], J. Seneca[26], N. Sennan[45], P. A. Sevle Myhr[41], I. Sgura[40], R. Shanidze[52], A. Sharma[16], Y. Shitov[21], F. Šimkovic[20], A. Simonelli[10], A. Sinopoulou[3], B. Spisso[10], M. Spurio[22,23], O. Starodubtsev[1], D. Stavropoulos[44], I. Štekl[21], D. Stocco[13], M. Taiuti[17,18], G. Takadze[52], Y. Tayalati[30,60], H. Thiersen[28], S. Thoudam[6], I. Tosta e Melo[3,39], B. Trocmé[16], V. Tsourapis[44], E. Tzamariudaki[44], A. Ukleja[51,57], A. Vacheret[19], V. Valsecchi[27], V. Van Elewyck[16,54], G. Vannoye[7,17,18], E. Vannuccini[1], G. Vasileiadis[62], F. Vazquez de Sola[26], A. Veutro[11,35], S. Viola[27], D. Vivolo[10,24], A. van Vliet[6], A. Y. Wen[15], E. de Wolf[26,33], I. Lhenry-Yvon[16], S. Zavatarelli[17], A. Zegarelli[11,35], D. Zito[27], J. D. Zornoza[8], J. Zúniga[8], and N. Zywucka[28]

(The KM3NeT Collaboration)

[1] INFN, Sezione di Firenze, via Sansone 1, Sesto Fiorentino, 50019, Italy
[2] Università di Firenze, Dipartimento di Fisica e Astronomia, via Sansone 1, Sesto Fiorentino, 50019, Italy
[3] INFN, Sezione di Catania, (INFN-CT) Via Santa Sofia 64, Catania, 95123, Italy
[4] Université de Strasbourg, CNRS, IPHC UMR 7178, F-67000 Strasbourg, France
[5] Université de Haute Alsace, rue des Frères Lumière, 68093 Mulhouse Cedex, France
[6] Khalifa University of Science and Technology, Department of Physics, PO Box 127788, Abu Dhabi, UAE
[7] Aix Marseille Univ, CNRS/IN2P3, CPPM, Marseille, France
[8] IFIC—Instituto de Física Corpuscular (CSIC—Universitat de València), c/Catedrático José Beltrán, 2, 46980 Paterna, Valencia, Spain
[9] Università di Napoli "Federico II," Dip. Scienze Fisiche "E. Pancini," Complesso Universitario di Monte S. Angelo, Via Cintia ed. G, Napoli, 80126, Italy; antonio.marinelli@na.infn.it
[10] INFN, Sezione di Napoli, Complesso Universitario di Monte S. Angelo, Via Cintia ed. G, Napoli, 80126, Italy
[11] INFN, Sezione di Roma, Piazzale Aldo Moro 2, Roma, 00185, Italy
[12] Universitat Politècnica de Catalunya, Laboratori d'Aplicacions Bioacústiques, Centre Tecnològic de Vilanova i la Geltrú, Avda. Rambla Exposició, s/n, Vilanova i la Geltrú, 08800, Spain
[13] Subatech, IMT Atlantique, IN2P3-CNRS, Nantes Université, 4 rue Alfred Kastler—La Chantrerie, Nantes, BP 20722 44307, France
[14] Universitat Politècnica de València, Instituto de Investigación para la Gestión Integrada de las Zonas Costeras, C/ Paranimf, 1, Gandia, 46730, Spain
[15] Harvard University, Department of Physics and Laboratory for Particle Physics and Cosmology, Lyman Laboratory, 17 Oxford St., Cambridge, MA 02138, USA
[16] Université Paris Cité, CNRS, Astroparticule et Cosmologie, F-75013 Paris, France; acondorelli@km3net.de
[17] INFN, Sezione di Genova, Via Dodecaneso 33, Genova, 16146, Italy
[18] Università di Genova, Via Dodecaneso 33, Genova, 16146, Italy
[19] LPC CAEN, Normandie Univ, ENSICAEN, UNICAEN, CNRS/IN2P3, 6 boulevard Maréchal Juin, Caen, 14050, France

[20] Comenius University in Bratislava, Department of Nuclear Physics and Biophysics, Mlynska dolina F1, Bratislava, 842 48, Slovak Republic
[21] Czech Technical University in Prague, Institute of Experimental and Applied Physics, Husova 240/5, Prague, 110 00, Czech Republic
[22] Università di Bologna, Dipartimento di Fisica e Astronomia, v.le C. Berti-Pichat, 6/2, Bologna, 40127, Italy
[23] INFN, Sezione di Bologna, v.le C. Berti-Pichat, 6/2, Bologna, 40127, Italy
[24] Università degli Studi della Campania "Luigi Vanvitelli," Dipartimento di Matematica e Fisica, viale Lincoln 5, Caserta, 81100, Italy
[25] E. A. Milne Centre for Astrophysics, University of Hull, Hull, HU6 7RX, UK
[26] Nikhef, National Institute for Subatomic Physics, PO Box 41882, Amsterdam, 1009 DB, The Netherlands
[27] INFN, Laboratori Nazionali del Sud, (LNS) Via S. Sofia 62, Catania, 95123, Italy
[28] North-West University, Centre for Space Research, Private Bag X6001, Potchefstroom, 2520, South Africa
[29] Université Badji Mokhtar, Département de Physique, Faculté des Sciences, Laboratoire de Physique des Rayonnements, B. P. 12, Annaba, 23000, Algeria
[30] University Mohammed V in Rabat, Faculty of Sciences, 4 av. Ibn Battouta, B.P. 1014, R.P. 10000 Rabat, Morocco
[31] Università di Salerno e INFN Gruppo Collegato di Salerno, Dipartimento di Fisica, Via Giovanni Paolo II 132, Fisciano, 84084, Italy
[32] Institute of Space Science - INFLPR Subsidiary, 409 Atomistilor Street, Magurele, Ilfov, 077125, Romania
[33] University of Amsterdam, Institute of Physics/IHEF, PO Box 94216, Amsterdam, 1090 GE, The Netherlands
[34] TNO, Technical Sciences, PO Box 155, Delft, 2600 AD, The Netherlands
[35] Università La Sapienza, Dipartimento di Fisica, Piazzale Aldo Moro 2, Roma, 00185, Italy
[36] Università di Bologna, Dipartimento di Ingegneria dell'Energia Elettrica e dell'Informazione "Guglielmo Marconi," Via dell'Università 50, Cesena, 47521, Italy
[37] Cadi Ayyad University, Physics Department, Faculty of Science Semlalia, Av. My Abdellah, P.O.B. 2390, Marrakech, 40000, Morocco
[38] University of the Witwatersrand, School of Physics, Private Bag 3, Johannesburg, Wits 2050, South Africa
[39] Università di Catania, Dipartimento di Fisica e Astronomia "Ettore Majorana," (INFN-CT) Via Santa Sofia 64, Catania, 95123, Italy
[40] INFN, Sezione di Bari, via Orabona, 4, Bari, 70125, Italy
[41] UCLouvain, Centre for Cosmology, Particle Physics and Phenomenology, Chemin du Cyclotron, 2, Louvain-la-Neuve, 1348, Belgium
[42] University of Granada, Department of Computer Engineering, Automation and Robotics/CITIC, 18071 Granada, Spain
[43] Friedrich-Alexander-Universität Erlangen-Nürnberg (FAU), Erlangen Centre for Astroparticle Physics, Nikolaus-Fiebiger-Straße 2, 91058 Erlangen, Germany
[44] NCSR Demokritos, Institute of Nuclear and Particle Physics, Ag. Paraskevi Attikis, Athens, 15310, Greece
[45] University Mohammed I, Faculty of Sciences, BV Mohammed VI, B.P. 717, R.P. 60000 Oujda, Morocco
[46] Western Sydney University, School of Computing, Engineering and Mathematics, Locked Bag 1797, Penrith, NSW 2751, Australia
[47] University of Granada, Dpto. de Física Teórica y del Cosmos & C.A.F.P.E., 18071 Granada, Spain
[48] NIOZ (Royal Netherlands Institute for Sea Research), PO Box 59, Den Burg, Texel, 1790 AB, The Netherlands
[49] Leiden University, Leiden Institute of Physics, PO Box 9504, Leiden, 2300 RA, The Netherlands
[50] AstroCeNT, Nicolaus Copernicus Astronomical Center, Polish Academy of Sciences, Rektorska 4, Warsaw, 00-614, Poland
[51] AGH University of Krakow, Al. Mickiewicza 30, 30-059 Krakow, Poland
[52] Tbilisi State University, Department of Physics, 3, Chavchavadze Ave., Tbilisi, 0179, Georgia
[53] The University of Georgia, Institute of Physics, Kostava str. 77, Tbilisi, 0171, Georgia
[54] Institut Universitaire de France, 1 rue Descartes, Paris, 75005, France
[55] Max-Planck-Institut für Radioastronomie, Auf dem Hügel 69, 53121 Bonn, Germany
[56] University of Sharjah, Sharjah Academy for Astronomy, Space Sciences, and Technology, University Campus—POB 27272, Sharjah, UAE
[57] National Centre for Nuclear Research, 02-093 Warsaw, Poland
[58] Faculty of Mathematics and Physics, Charles University in Prague, Prague, Czech Republic
[59] Harvard University, Black Hole Initiative, 20 Garden St., Cambridge, MA 02138, USA
[60] School of Applied and Engineering Physics, Mohammed VI Polytechnic University, Ben Guerir, 43150, Morocco
[61] University of Johannesburg, Department Physics, PO Box 524, Auckland Park, 2006, South Africa
[62] Laboratoire Univers et Particules de Montpellier, Place Eugène Bataillon—CC 72, Montpellier Cédex 05, 34095, France
Received 2025 February 14; revised 2025 April 4; accepted 2025 April 12; published 2025 May 2

Abstract

On 2023 February 13, the KM3NeT/ARCA telescope observed a track-like event compatible with a ultra-high-energy muon with an estimated energy of 120 PeV, produced by a neutrino with an even higher energy, making it the most energetic neutrino event ever detected. A diffuse cosmogenic component is expected to originate from the interactions of ultra-high-energy cosmic rays with ambient photon and matter fields. The flux level required by the KM3NeT/ARCA event is, however, in tension with the standard cosmogenic neutrino predictions based on the observations collected by the Pierre Auger Observatory and Telescope Array over the last decade of the ultra-high-energy cosmic rays above the ankle (hence from the local Universe, $z \lesssim 1$). We show here that both observations can be reconciled by extending the integration of the equivalent cosmogenic neutrino flux up to a redshift of $z_{\rm max} = 6$ and considering either source evolution effects or the presence of a subdominant independent proton component in the ultra-high-energy cosmic-ray flux, thus placing constraints on known cosmic accelerators.

Unified Astronomy Thesaurus concepts: Ultra-high-energy cosmic radiation (1733); Non-thermal radiation sources (1119); Neutrino astronomy (1100)

1. Introduction

The presence of extreme cosmic accelerators in our Universe has been established in recent decades by the observation of gamma rays, cosmic rays, and neutrinos (W. B. Atwood et al. 2009; M. G. Aartsen et al. 2013; A. Aab et al. 2015). A multimessenger approach aims to combine detections of various cosmic messengers to overcome observational limitations and unveil the underlying astrophysical processes in a source environment or in the extragalactic medium. However,

[63] Corresponding author.
[64] Deceased.

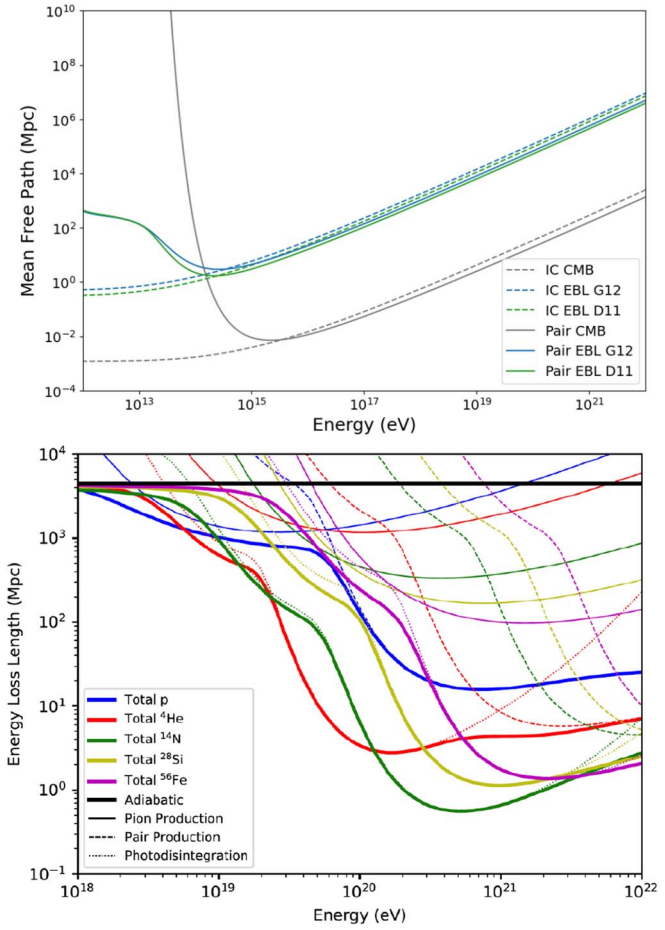

Figure 1. Top: mean free path of photons as a function of energy. Pair production (Pair) and inverse-Compton (IC) interactions with photons of the CMB and EBL (for two different models) are shown. Bottom: energy loss length of protons and nuclei as a function of energy. Different interactions with photons of the CMB and EBL are considered. The plots have been made using the CRPropa (R. Alves Batista et al. 2022) software.

the distant Universe remains unexplored at the highest energies because it is opaque to both cosmic rays and gamma rays. Gamma rays with energies exceeding a few TeV interact with low-energy photons of the extragalactic background light (EBL; J. D. Finke et al. 2010; A. Domínguez et al. 2011) or cosmic microwave background (CMB; N. Aghanim et al. 2020), resulting in e^+e^- pair production, which severely attenuates their propagation over cosmological distances, as shown in the top panel of Figure 1. Similarly, cosmic rays at the highest energies ($\geqslant 10^{18}$ eV) suffer energy losses and photodisintegration through interactions with CMB and EBL photons (V. Berezinsky et al. 2006), resulting in a mean free path smaller than a few Gpc (which corresponds to a redshift $z \simeq 1$), as shown in the bottom panel of Figure 1. At lower energies, charged nuclei are also deflected by the ambient magnetic fields, which further impedes the identification of their sources. In contrast to the other messengers, neutrinos interact only weakly with matter and radiation, allowing them to travel virtually unimpeded over cosmological distances. This makes neutrinos invaluable probes of the most remote and densest regions of the Universe, where other messengers are absorbed or scattered. The detection of ultra-high-energy (UHE) neutrinos could therefore constitute a unique proof of the presence of extreme accelerators in the faraway Universe.

This work investigates the possibility that the neutrino event (KM3-230213A) observed in KM3NeT/ARCA with an energy in the 90% confidence level (CL) range (72 PeV–2.6 EeV) is a cosmogenic neutrino produced in a region of the Universe deep enough to account for the estimated neutrino flux. In S. Aiello et al. (2025), a wide range of cosmogenic models has been presented (see Table 4 of S. Aiello et al. 2025): some minimal scenarios (D. Boncioli et al. 2019; J. Heinze et al. 2019; C. Bérat 2023; A. Condorelli et al. 2023) predict a very low cosmogenic neutrino flux. Other works instead result in more optimistic expectations (R. Aloisio et al. 2015; B. T. Zhang & K. Murase 2019; A. A. Halim et al. 2023; M. S. Muzio et al. 2023; D. Ehlert et al. 2024) by considering, for example, the interplay between two source populations. In this work, a fit of cosmic-ray data at the highest energies is performed, illustrating how the expected flux can be enhanced starting from a minimal scenario. The Letter is organized as follows. In Section 2, cosmogenic neutrinos and their importance for multimessenger astronomy are described. In Section 3, KM3-230213A as observed by the KM3NeT/ARCA detector is detailed. Using the inputs of Sections 2 and 3, the adopted cosmological scenario is reported in Section 4, and the spectra produced in the nearby and faraway Universe are compared in Section 5. Finally, the significance of the results is discussed in Section 7.

2. Cosmogenic Neutrinos

The energy spectrum of cosmic rays has been observed to extend beyond 10^{20} eV (J. Linsley 1963), indicating that charged particles can be accelerated to ultrahigh energies in powerful astrophysical objects, although their exact sources remain unidentified. The interaction processes involving UHE cosmic rays (UHECRs) and background photons in the Universe include pair production and photopion production for protons, as well as photodisintegration for heavier nuclei. When nucleons undergo photopion production, they generate pions. The decay of charged pions (and the associated muons) produced by photopion production leads to the production of a large number of neutrinos, referred to as cosmogenic neutrinos. UHE neutrinos are predicted to arise from the interactions of cosmic rays with background photon fields permeating the Universe. This mechanism, extensively studied in the literature (e.g., C. T. Hill & D. N. Schramm 1985; R. J. Protheroe & P. A. Johnson 1996; S. Lee 1998; E. Waxman & J. N. Bahcall 1999; R. Engel et al. 2001; M. Ahlers et al. 2010; K.-H. Kampert & B. Sarkar 2011; A. A. Halim et al. 2023; C. Petrucci et al. 2023), relies on several assumptions, leading to flux predictions that can vary by orders of magnitude. The dominant production channel involves the decay of $\pi^{\pm}$ mesons, created by primary proton cosmic rays or secondary nucleons produced during the photodisintegration of nuclei interacting with background photons. As nucleons inherit a fraction of the fragmented nucleus energy, neutrinos from heavier nuclei tend to have lower energies than those from lighter nuclei or protons. Consequently, the cosmogenic neutrino flux is strongly dependent on the cosmic-ray mass composition, which is poorly constrained above 5×10^{19} eV (E. W. Mayotte et al. 2023). Other key factors include the maximum acceleration energy, the shape of the particle energy spectrum, and the cosmological evolution of their sources. Advances in constraining these parameters have significantly altered flux predictions at 10^{18} eV: initial estimates of $E^2\phi_\nu \sim 10^{-9}$ GeV cm^{-2} sr^{-1} s^{-1}, assuming a pure-proton composition, have dropped to $E^2\phi_\nu \sim 10^{-12}$ GeV cm^{-2} sr^{-1} s^{-1} under

mixed-composition models, consistent with data from the Pierre Auger Observatory (A. Aab et al. 2014a, 2014b; O. Tkachenko et al. 2023) and other experiments (A. A. Watson 2022).

Finally, cosmogenic neutrinos can also be produced through interactions between UHE particles and interstellar matter in the Galactic disk. This mechanism mirrors the production of lower-energy neutrinos recently observed from Galactic cosmic rays (R. Abbasi et al. 2023a). Interactions of UHECRs within our Galaxy provide a guaranteed baseline for cosmogenic neutrino production (C. Bérat et al. 2024). The procedure to compute cosmogenic neutrino fluxes is detailed in Section 4.

3. KM3-230213A

A UHE muon traversing the KM3NeT/ARCA detector was observed on 2023 February 13 at 01:16:47 UTC (KM3-230213A). At that time, 21 detection units were in operation. The detector, referred to as ARCA21, collected data in this configuration from 2022 September 23 until 2023 September 11, for a total livetime T^{ARCA21} of 287.4 days. Over this period, about 110 million events were triggered, with KM3-230213A being the highest-energy event observed. The estimated muon energy is 120^{+110}_{-60} PeV, with a 90% CL interval of 35–380 PeV, while the corresponding median neutrino energy to produce such a muon in the simulations of the ARCA detector is 220 PeV; the 68% (90%) of simulated events fall in the 110−790 PeV (72 PeV−2.6 EeV) energy range. The KM3NeT collaboration explored the compatibility of this event with nonobservations by IceCube and Auger in this work (O. Adriani et al. 2025), finding a 0.5% (2.6σ) probability of detecting one event in KM3NeT and none in the others, which does not rule out a diffuse flux.

4. Description of the Cosmogenic Scenario

4.1. Injected Cosmic-Ray Composition

The nonthermal processes responsible for accelerating the different types of particles are usually modeled using power-law spectra, while an exponential suppression is used to describe the end of the acceleration process in the absence of any strong indication from theory. Sources are believed to accelerate diverse proportions of nuclei, which, for simplicity, are grouped into five stable representative nuclei: hydrogen (^{1}H), helium (^{4}He), nitrogen (^{14}N), silicon (^{28}Si), and iron (^{56}Fe). The ejection rate $q_A(E)$ of nuclei with mass number A per comoving unit volume and per unit energy of nucleons is usually modeled as

$$q_A(E) = q_{0A}\left(\frac{E}{E_0}\right)^{-\gamma_A} f(E, Z_A), \tag{1}$$

where γ_A is the spectral index and q_{0A} are the injection rates. The suppression function used for nucleons and nuclei is the same as in the reference case of A. Aab et al. (2017a):

$$f(E, Z) = \begin{cases} 1 & \text{if} \quad E \leqslant E^{Z}_{\mathrm{max}}, \\ \exp\left(1 - E/E^{Z}_{\mathrm{max}}\right) & \text{otherwise.} \end{cases} \tag{2}$$

The maximum acceleration energy is expected to be proportional to the electric charge of each element, $E^{Z}_{\mathrm{max}} = ZE_{\mathrm{max}}$, where E_{max} is a single free parameter.

For each atomic species A, the differential energy production rate per comoving volume unit of the sources, which is directly connected to their differential luminosity, is consequently

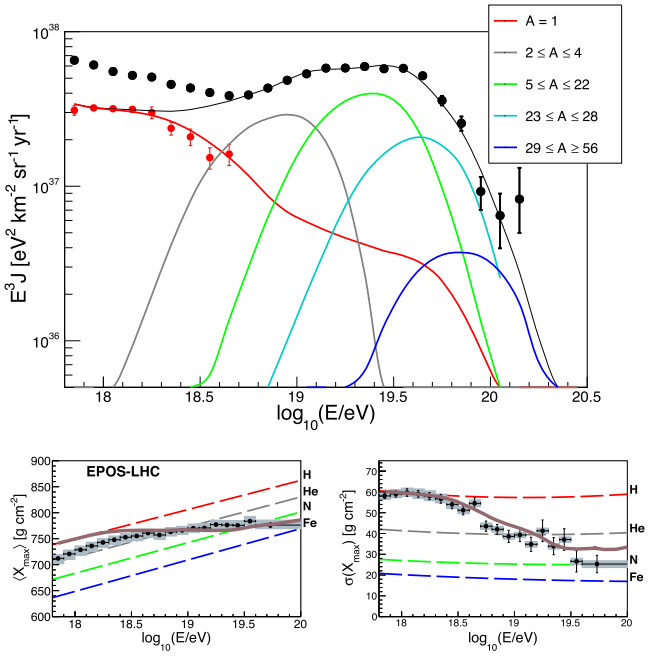

Figure 2. Top: energy flux at Earth as a function of energy, as modeled by the best-fit parameters for the benchmark scenario. The all-particle spectrum (from P. Abreu et al. 2021) and proton component (using the proton fraction as published in O. Tkachenko et al. 2023) are shown as black and red circles, respectively. Points below the energy of the ankle ($E = 10^{18.7}$ eV) are not included in the fit procedure. Bottom: average (left panel) and standard deviation (right panel) of the experimental (black dots as reported in T. Fitoussi et al. 2023) and expected (lines) X_{max} distributions.

$\ell_A(E, z) = E^2 q_A(E) S(z)$, where $S(z)$ reflects the redshift evolution of the UHECR luminosity density. The bolometric energy production rate per comoving volume unit at redshift z, on the other hand, is calculated as

$$\mathcal{L}_A(E, z) = S(z) \int_E^{\infty} dE' E' q_A(E'). \tag{3}$$

The energy spectrum is described using $\log_{10}(E/\mathrm{eV})$ bins with a width of 0.1, spanning from 17.8 to 20.2. This measurement is based on 15 yr of data collected with the surface detector array of the Pierre Auger Observatory (A. Aab et al. 2020). To present the X_{max} distributions (A. Aab et al. 2014b), $\log_{10}(E/\mathrm{eV})$ bins of 0.1 from 17.8 to 19.6 are used, with an additional, broader bin including events with energies above $10^{19.6}$ eV. Each X_{max} distribution is divided into intervals of 20 g cm^{-2}. The agreement between the model described in this Letter and the UHECR data is evaluated following the procedure outlined in A. Aab et al. (2017b). As an example, Figure 2 illustrates the spectrum and mass composition of UHECRs at Earth relative to the best-fit scenario in Section 6.

4.2. Cosmological Source Evolution

The bulk of UHECRs detected by the Pierre Auger Observatory (P. Abreu et al. 2021) and the Telescope Array (R. Abbasi et al. 2023b) as well as their measured spectra are mostly driven by nearby astrophysical accelerators, implying that UHE-related source properties are mostly unexplored for $z \geqslant 1$. Different astrophysical candidates, steady or transients, can accelerate cosmic rays up to 10^{21} eV when extreme environments are considered, among them different classes of active galactic nuclei (AGN; V. Berezinsky et al. 2006; R. Blandford et al. 2019), starburst galaxies (A. M. Bykov et al. 2020), gamma-ray bursts

(M. Vietri 1995), and tidal disruption events (C. Guépin et al. 2018; P. Plotko et al. 2024). Their comoving source density is generally parameterized as

$$S(z) \propto (1+z)^m. \tag{4}$$

In this work, m is varied from -5 to 5 with a step of 0.2, covering all possible source evolution scenarios without assuming a specific source type. At low redshifts ($z \lesssim 1$), a strong positive evolution ($m = 5$) could correspond to high-luminosity sources, such as jetted objects, e.g., blazars, observed in gamma rays (M. Ajello et al. 2014), or nonjetted sources like high-luminosity Seyfert galaxies (Y. Ueda et al. 2014). A weaker positive evolution ($m = 3$) aligns with the star formation rate (SFR) evolution (P. Madau & M. Dickinson 2014). Flat evolution ($m = 0$) may be linked to the stellar mass density in the Universe (Y. Fukazawa et al. 2022), low-luminosity Seyfert galaxies in X-rays (C. S. Kochanek 2016), or intermediate-luminosity BL Lacs and FSRQs (M. Ajello et al. 2014). Negative evolutions ($m = -3$) are associated with low-luminosity BL Lacs (M. Ajello et al. 2014), radio galaxies (Y. Fukazawa et al. 2022), or the redshift evolution of tidal disruption events (C. S. Kochanek 2016). At higher redshifts ($z \gtrsim 1$), the evolution of some of these source classes remains uncertain.

The resulting flux of cosmogenic neutrinos can vary with distance, depending on the assumed source evolution. The emission rate density $L(E, z)$ of cosmic rays per comoving volume for different accelerator populations can be expressed as

$$L(E, z) = S(z) \times Q_{\rm CR}(E), \tag{5}$$

where $Q_{\rm CR}(E)$ represents the injection term for the source type, and it is the sum of the injection terms $q_A(E)$ for each mass introduced in Equation (1). The implications of this assumption and its associated uncertainties are discussed in Section 7.

5. Expected Neutrino Fluxes for Different Redshift

Using this framework, a scan over plausible source evolutions parameterized as in Equation (4) with m ranging from -5 to 5 has been performed. The cosmogenic neutrino fluxes associated with the best-fit parameters that describe the UHECR energy spectrum and composition are shown in Figure 3. In the top panel, we limit the UHECR source distribution up to redshift $z_{\rm max} = 1$, which represents the distance beyond which UHECRs above the so-called ankle are expected to interact significantly. In the bottom panel, the source distribution has been extended up to redshift $z_{\rm max} = 6$, considering that the Universe is opaque to high-energy neutrinos at early times (V. S. Berezinsky 1992; P. Gondolo et al. 1993).

In both cases, the neutrino fluxes exhibit two distinct bumps in the energy range of interest, corresponding to interactions with the EBL at lower energies and the CMB at higher energies. A noticeable change of shape can be observed when transitioning from negative to positive source evolution, as reflected in the plots, where violet tones predominantly represent the former and yellow tones the latter. This effect arises from transitioning between regions of parameter space where a negligible quantity of protons is predicted to configurations that are proton-rich. Negative source evolution

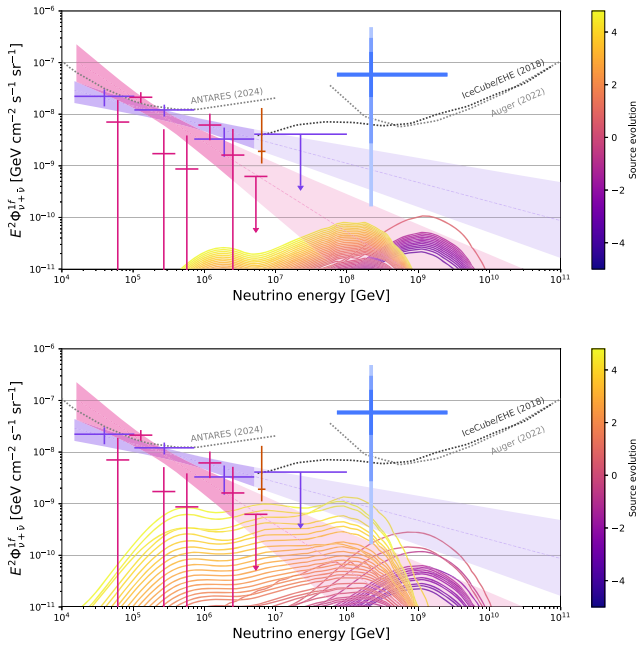

Figure 3. Expected neutrino fluxes as a function of energy for different source evolutions (color code) for two different maximum redshift values: $z_{\rm max} = 1$ (top panel) and $z_{\rm max} = 6$ (bottom panel). The blue cross corresponds to the flux needed to produce one expected event in the central 90% CL range of neutrino energy associated with the KM3-230213A event (horizontal span); the vertical bars represent the 1σ, 2σ, and 3σ Feldman–Cousins confidence intervals on this estimate (S. Aiello et al. 2025). The purple and pink shaded regions represent the 68% CL contours of the IceCube single power-law fits (northern sky tracks and high-energy starting events, respectively): the darker shaded regions are the respective 90% central energy range at the best fit (dashed line), while the lighter shaded regions are extrapolations to higher energies. The purple and pink crosses are the fits from the same analyses, while the orange cross corresponds to the IceCube Glashow resonance event. The dotted lines are upper limits from ANTARES (95% CL), Pierre Auger, and IceCube.

implies that the total flux is dominated by nearby sources, which provides less room for photodisintegration of heavy nuclei. Consequently, the fit favors an intermediate-mass composition at the source, closely resembling what is observed at Earth. In contrast, a positive evolution parameter suggests that most sources are farther away, allowing more photodisintegration processes. This enables a heavier composition at the source, which becomes lighter at Earth due to interactions in the interstellar medium. As a result, the neutrino flux associated with positive source evolution is more abundant in both cases of $z_{\rm max} = 1$ and $z_{\rm max} = 6$. During this process, a significant number of protons are produced, which play a critical role in neutrino production, as will be further discussed in the following section.

The two panels of Figure 3 show that for the $z_{\rm max} = 1$ scenario, the fluxes remain below $10^{-10}\,{\rm GeV\,cm^{-2}\,s^{-1}\,sr^{-1}}$ in the energy of interest. In contrast, considering sources at higher redshifts ($z_{\rm max} = 6$) can lead to an increase of the cosmogenic flux by about 1 order of magnitude, suggesting that, if the observed neutrino is cosmogenic, it is more likely to originate from distant sources rather than being associated with the UHECR flux measured above the ankle. The expected number of events $n_{\rm exp}$ for a specific flux model $\Phi_{\rm model}$ is evaluated as

$$n_{\rm exp}^{\rm ARCA21} = T^{\rm ARCA21} \sum_i \int_{\Delta\Omega_i} \int_{\Delta E} A_{\rm eff}^{\rm ARCA21}(E, \Omega) \times \Phi_{\rm model}(E, \Omega)\, dE\, d\Omega, \tag{6}$$

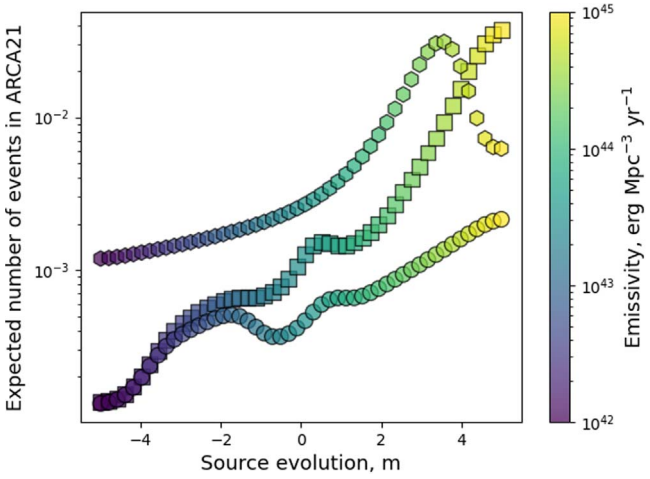

Figure 4. Expected number of events in ARCA21 as a function of source evolution for $z_{\max} = 1$ (circles) and $z_{\max} = 6$ (squares) in a minimal scenario and in the case of an additional proton component (hexagons). The displayed trend has been smoothed using a Gaussian to enhance continuity. The color axis represents the emissivity of plausible cosmic-ray sources.

where $A_{\rm eff}^{\rm ARCA21}$ represents the effective areas for events in different ranges of the zenith angle $\Delta\Omega_i$. For each flux model, the expected event rate in ARCA21 is calculated by integrating over the full energy range as in S. Aiello et al. (2025), including the region above 100 PeV. The effective area is computed using the same selections as adopted in S. Aiello et al. (2025).

The computed neutrino fluxes can then be translated into the expected number of events. Using Equation (6), the expected number of events has been evaluated for various source evolutions, considering two scenarios: $z_{\max} = 1$ and $z_{\max} = 6$. The results are shown in Figure 4 (squares and circles): for negative values of m, the two scenarios are nearly indistinguishable due to the very low neutrino flux. However, as m increases, the distinction between nearby and distant Universe scenarios becomes evident, with significantly more events expected in the $z_{\max} = 6$ case.

Furthermore, the parameter space regions that best describe our observations are those with higher m values, indicating higher emissivity (see color axis in Figure 4), where the emissivity is defined as the luminosity density needed to power the UHECR spectrum at $z = 0$ and computed as shown in Equation (3). This result is expected, as positive m values imply more interactions, and, consequently, the power of the accelerators must be higher in these scenarios.

Different extragalactic objects can be identified as UHECR accelerators considering their physical properties mainly derived through electromagnetic observations. Even though such properties can be assumed to remain similar for a significant fraction of the history of the Universe (P. Jakobsson et al. 2006), it is important to probe the efficiency and cosmological evolution of UHE accelerators up to high redshift through UHE astrophysical messengers. The observation of KM3-230213A gives the possibility to explore a new region of the Universe in the energy range of 10^{17}–10^{18} eV for ν (therefore up to 10^{20} eV for cosmic rays) so far untested by the Pierre Auger and Telescope Array observatories. It would be valuable to compare the emissivity values reported in the color axis of Figure 4 with those of plausible source candidates. However, it is crucial to emphasize that the reported values represent emissivity in cosmic rays, while source emissivity is typically expressed in terms of gamma rays or electromagnetic emission. As a result, a direct comparison is not straightforward without applying a conversion factor to estimate the fraction of energy channeled into cosmic rays relative to the electromagnetic component.

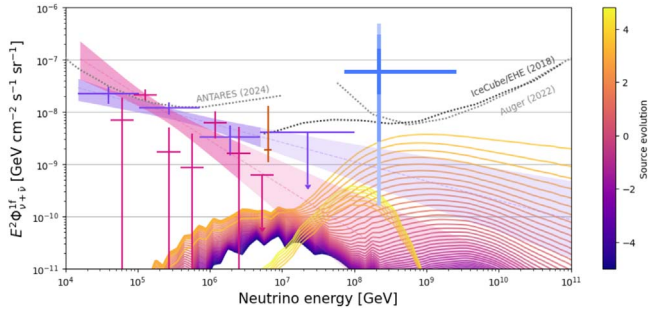

Figure 5. Expected neutrino fluxes as a function of energy assuming a second component, made of protons, subdominant at the highest energies. The figure follows the same format as Figure 3.

6. Constraining the Proton Fraction at the Highest Energies

Protons are significantly more effective than nuclei in producing pions and high-energy neutrinos, as they interact efficiently with photon fields (primarily the CMB at the highest energies) through photopion production ($p + \gamma \rightarrow \Delta^+ \rightarrow \pi + N$), generating charged pions that decay into neutrinos. The photopion production process also holds for nucleons bound within UHE nuclei, being the interacting nucleon ejected from the parent nucleus, but this process is subdominant with respect to nucleus photodisintegration except at extremely high energies. Thus, compared to nuclei, protons contribute more significantly to pion production, and consequently to neutrino production, at high energies.

Recent works (G. Decerprit & D. Allard 2011; M. S. Muzio et al. 2019; A. A. Halim et al. 2023; D. Ehlert et al. 2024) have demonstrated that the inclusion of a proton component, while preserving the expected mass composition (predominantly intermediate masses), can significantly influence the predicted neutrino flux.

This scenario has been explored within the cosmogenic framework by introducing a secondary component, made only by protons, with a different spectral index in order to fit the proton fraction mass composition as measured by the Pierre Auger Observatory. This was implemented by fitting the energy spectrum and mass composition data below the ankle, using the proton spectrum measured by Auger, and extrapolating it to the highest energies.

The resulting neutrino flux predictions are shown in Figure 5, highlighting how the presence of a subdominant proton component can enhance the expected neutrino flux.

In conclusion, even a small fraction of protons at the highest energies translates into a significant increase of the cosmogenic neutrino flux, which can offer prospects for more future detections (X. Rodrigues et al. 2021; A. A. Halim et al. 2023; M. S. Muzio et al. 2023). The observation of KM3-230213A can then support the possibility of a subdominant proton component at the highest energies, assuming the cosmogenic hypothesis.

7. Discussion

The observation of KM3-230213A has triggered the investigation of its possible origin as a cosmogenic neutrino, based on the existence of known cosmic accelerators and the available observations of UHECRs. The cosmogenic origin is compatible (0.06 expected events for the most optimistic scenario for the lifetime of ARCA21, which corresponds to a probability of 5.6% to observe an event) with the reported neutrino flux when looking into the deep sky ($z_{\max} \simeq 6$) and at strong positive cosmological source evolution, allowing for a nonnegligible proton fraction at the highest energies, modeled as a subdominant, independent proton component up to the highest energies.

In this work, results have been presented using a simple source evolution $S(z) \propto (1 + z)^m$ with constant m across the entire redshift z range. However, possible improvements to the model include exploring alternative assumptions, such as aligning the UHECR production rate in the Universe with the SFR (P. Madau & M. Dickinson 2014). This idea stems from the premise that a higher rate of astrophysical explosions correlates with increased production of cosmic rays at the highest energies.

According to trends in the literature, the SFR evolution is parameterized with a functional form, which features a rise at low redshifts, a plateau at intermediate redshifts, and a decline at high redshifts, following the parametric formula as reported in R. Aloisio et al. (2015). It is found that the neutrino flux associated with a population evolving as the SFR history is significantly lower with respect to the one obtained with a simplified source evolution shown in the bottom panel of Figure 3. An analogous approach has been considered by assuming an AGN-like evolution (M. Ahlers et al. 2009). Despite a more abundant flux ($\simeq$2 times more abundant) with respect to the SFR one, the neutrino flux is still much lower than the ones shown in the previous section, using the evolution reported in Equation (4). From these results it is possible to conclude that, if the origin of KM3-230213A is cosmogenic, the UHE production rate should not follow the distribution of matter so far known. Conversely, it also implies that either a subdominant proton component or a strong source evolution is necessary to provide such abundant flux at the highest energies.

Previous studies found that differences between EBL models had a nonnegligible impact in UHECR propagation (R. Alves Batista et al. 2015). Nonetheless, over the last few years, recent EBL models have been updated. Four of them have been tested: Gilmore (R. C. Gilmore et al. 2012), Dominguez (A. Domínguez et al. 2011), Saldana-Lopez (A. Saldana-Lopez et al. 2021), and Andrews (S. K. Andrews et al. 2018). The uncertainties induced by the EBL models are found to be smaller than the systematic uncertainties on the energy spectrum and mass composition. Therefore, it can be concluded that the uncertainties on the EBL model do not influence the main message of this Letter.

The impact of the photodisintegration cross-section model has also been investigated. Two different models have been used, PSB (J. L. Puget et al. 1976) and A. J. Koning et al. (2005), with the latter being employed in this analysis. It is observed that the differences in the proton fraction are on the order of 5%, which has a negligible impact on the expected cosmogenic neutrino flux. Thus, these two sources of uncertainty in the modeling do not compromise the main conclusions of this work.

8. Conclusion

In this study, the cosmogenic origin of KM3-230213A has been investigated with the aim of understanding the source features and the implications for high-energy astrophysical processes. In this work, we show that, following the cosmogenic hypothesis, the theoretical models favor strong evolutions of the sources and a nonnegligible proton fraction produced at the highest energies. At the same time, an additional diffuse extragalactic component is plausible, accounting for neutrinos produced in the source environment. This aligns with the expectation that at the highest energies, the observed neutrino flux is not entirely cosmogenic; instead, it likely includes contributions from various astrophysical sources. In the future, KM3NeT sensitivity at the highest energies will enable more precise constraints on the expected cosmogenic fluxes, being competitive with the sensitivities achieved by other experiments (A. Aab et al. 2019; R. Abbasi et al. 2022). While uncertainties in UHECR source modeling persist, advancements in neutrino detection capabilities are expected to further refine the understanding of UHE neutrino production. In doing so, they offer complementary insights that contribute to completing the multimessenger astrophysics puzzle. Ultimately, this work highlights the potential of high-energy neutrino astronomy as a key probe for observing the most distant high-energy cosmic-ray accelerators, a task that will be further advanced by the capabilities of the KM3NeT telescope.

Acknowledgments

The authors acknowledge the financial support of the KM3NeT-INFRADEV2 project, funded by the European Union Horizon Europe Research and Innovation Programme under grant agreement No. 101079679; Funds for Scientific Research (FRS-FNRS), Francqui foundation, BAEF foundation; Czech Science Foundation (GAČR 24-12702S); Agence Nationale de la Recherche (contract ANR-15-CE31-0020), Centre National de la Recherche Scientifique (CNRS), Commission Européenne (FEDER fund and Marie Curie Program), LabEx UnivEarthS (ANR-10-LABX-0023 and ANR-18-IDEX-0001), Paris Île-de-France Region, Normandy Region (Alpha, Blue-waves and Neptune), France, the Provence-Alpes-Côte d'Azur Delegation for Research and Innovation (DRARI), the Provence-Alpes-Côte d'Azur region, the Bouches-du-Rhône Departmental Council, the Metropolis of Aix-Marseille Provence and the City of Marseille through the CPER 2021-2027 NEUMED project, the CNRS Institut National de Physique Nucléaire et de Physique des Particules (IN2P3); Shota Rustaveli National Science Foundation of Georgia (SRNSFG, FR-22-13708), Georgia.

This work is part of the MuSES project, which has received funding from the European Research Council (ERC) under the European Union's Horizon 2020 Research and Innovation Programme (grant agreement No. 101142396). This work was supported by the European Research Council, ERC starting grant *MessMapp*, under contract No. 949555. The General Secretariat of Research and Innovation (GSRI), Greece; Istituto Nazionale di Fisica Nucleare (INFN) and Ministero dell'Università e della Ricerca (MUR), through PRIN 2022 program (Grant PANTHEON

2022E2J4RK, Next Generation EU) and PON R&I program (Avviso n. 424 del 28 febbraio 2018, Progetto PACK-PIR01 00021), Italy; IDMAR project Po-Fesr Sicilian Region az. 1.5.1; A.D.B., W.I.I., M.B., A.N., G.P., I.C.R., and A.S. have been supported by the Italian Ministero dell'Università e della Ricerca (MUR), Progetto CIR01 00021 (Avviso n. 2595 del 24 dicembre 2019); KM3NeT4RR MUR Project National Recovery and Resilience Plan (NRRP), Mission 4 Component 2 Investment 3.1, Funded by the European Union—NextGenerationEU,CUP I57G21000040001, Concession Decree MUR No. n. Prot. 123 del 21/06/2022; Ministry of Higher Education, Scientific Research and Innovation, Morocco, and the Arab Fund for Economic and Social Development, Kuwait; Nederlandse organisatie voor Wetenschappelijk Onderzoek (NWO), the Netherlands; The grant "AstroCeNT: Particle Astrophysics Science and Technology Centre," carried out within the International Research Agendas program of the Foundation for Polish Science financed by the European Union under the European Regional Development Fund; The program: "Excellence initiative-research university" for the AGH University in Krakow; The ARTIQ project: UMO-2021/01/2/ST6/00004 and ARTIQ/0004/2021; Ministry of Research, Innovation and Digitalisation, Romania; Slovak Research and Development Agency under contract No. APVV-22-0413; Ministry of Education, Research, Development and Youth of the Slovak Republic; MCIN for PID2021-124591NB-C41, -C42, -C43 and PDC2023-145913-I00 funded by MCIN/AEI/10.13039/501100011033 and by "ERDF A way of making Europe," for ASFAE/2022/014 and ASFAE/2022 /023 with funding from the EU NextGenerationEU (PRTR-C17.I01) and Generalitat Valenciana, for grant AST22_6.2 with funding from Consejería de Universidad, Investigación e Innovación and Gobierno de España and European Union—NextGenerationEU, for CSIC-INFRA23013 and for CNS2023-144099, Generalitat Valenciana for CIDEGENT/2018/034, /2019/043, /2020/049, /2021/23, for CIDEIG/2023/20, for CIPROM/2023/51 and for GRISOLIAP/2021/192 and EU for MSC/101025085, Spain; Khalifa University internal grants (ESIG-2023-008, RIG-2023-070 and RIG-2024-047), United Arab Emirates; the European Union's Horizon 2020 Research and Innovation Programme (ChETEC-INFRA—Project No. 101008324).

ORCID iDs

A. Condorelli https://orcid.org/0000-0001-5681-0086

References

Aab, A., Abreu, P., Aglietta, M., et al. 2014a, PhRvD, 90, 122006
Aab, A., Abreu, P., Aglietta, M., et al. 2014b, PhRvD, 90, 122005
Aab, A., Abreu, P., Aglietta, M., et al. 2015, NIMPA, 798, 172
Aab, A., Abreu, P., Aglietta, M., et al. 2017a, JCAP, 04, 038
Aab, A., Abreu, P., Aglietta, M., et al. 2017b, JCAP, 2017, 038
Aab, A., Abreu, P., Aglietta, M., et al. 2019, JCAP, 11, 004
Aab, A., Abreu, P., Aglietta, M., et al. 2020, PhRvL, 125, 121106
Aartsen, M. G., Abbasi, R., Abdou, Y., et al. 2013, Sci, 342, 1242856
Abbasi, R., Ackermann, M., Adams, J., et al. 2022, JCAP, 2023, 003
Abbasi, R., Ackermann, M., Adams, J., et al. 2023a, Sci, 380, 1338
Abbasi, R., Abe, Y., Abu-Zayyad, T., et al. 2023b, APh, 151, 102864
Abreu, P., Aglietta, M., Albury, J. M., et al. 2021, EPJC, 81, 966
Adriani, O., Aiello, S., Albert, A., et al. 2025, arXiv:2502.08173
Aghanim, N., Akrami, Y., Ashdown, M., et al. 2020, A&A, 641, A6
Ahlers, M., Anchordoqui, L. A., Gonzalez-Garcia, M. C., Halzen, F., & Sarkar, S. 2010, APh, 34, 106
Ahlers, M., Anchordoqui, L. A., & Sarkar, S. 2009, PhRvD, 79, 083009
Aiello, S., Albert, A., Alhebsi, A. R., et al. 2025, Natur, 638, 376
Ajello, M., Romani, R. W., Gasparrini, D., et al. 2014, ApJ, 780, 73
Aloisio, R., Boncioli, D., di Matteo, A., et al. 2015, JCAP, 10, 006
Alves Batista, R., Boncioli, D., di Matteo, A., van Vliet, A., & Walz, D. 2015, JCAP, 10, 063
Alves Batista, R., Becker Tjus, J., Dörner, J., et al. 2022, JCAP, 09, 035
Andrews, S. K., Driver, S. P., Davies, L. J. M., Lagos, C. d. P., & Robotham, A. S. G. 2018, MNRAS, 474, 898
Atwood, W. B., Abdo, A. A., Ackermann, M., et al. 2009, ApJ, 697, 1071
Bérat, C. 2023, EPJWC, 283, 06001
Bérat, C., Condorelli, A., Deligny, O., Montanet, F., & Torrès, Z. 2024, ApJ, 966, 186
Berezinsky, V., Gazizov, A. Z., & Grigorieva, S. I. 2006, PhRvD, 74, 043005
Berezinsky, V. S. 1992, NuPhB, 380, 478
Blandford, R., Meier, D., & Readhead, A. 2019, ARA&A, 57, 467
Boncioli, D., Biehl, D., & Winter, W. 2019, ApJ, 872, 110
Bykov, A. M., Marcowith, A., Amato, E., et al. 2020, SSRv, 216, 42
Condorelli, A., Boncioli, D., Peretti, E., & Petrera, S. 2023, PhRvD, 107, 083009
Decerprit, G., & Allard, D. 2011, A&A, 535, A66
Domínguez, A., Primack, J. R., Rosario, D. J., et al. 2011, MNRAS, 410, 2556
Ehlert, D., van Vliet, A., Oikonomou, F., & Winter, W. 2024, JCAP, 02, 022
Engel, R., Seckel, D., & Stanev, T. 2001, PhRvD, 64, 093010
Finke, J. D., Razzaque, S., & Dermer, C. D. 2010, ApJ, 712, 238
Fitoussi, T., Abdul Halim, A., Abreu, P., et al. 2023, ICRC (Nagoya), 444, 319
Fukazawa, Y., Matake, H., Kayanoki, T., et al. 2022, ApJ, 931, 138
Gilmore, R. C., Somerville, R. S., Primack, J. R., & Dominguez, A. 2012, MNRAS, 422, 3189
Gondolo, P., Gelmini, G., & Sarkar, S. 1993, NuPhB, 392, 111
Guépin, C., Kotera, K., Barausse, E., Fang, K., & Murase, K. 2018, A&A, 616, A179
Halim, A. A., Abreu, P., Aglietta, M., et al. 2023, JCAP, 05, 024
Heinze, J., Fedynitch, A., Boncioli, D., & Winter, W. 2019, ApJ, 873, 88
Hill, C. T., & Schramm, D. N. 1985, PhRvD, 31, 564
Jakobsson, P., Levan, A., Fynbo, J. P. U., et al. 2006, A&A, 447, 897
Kampert, K.-H., & Sarkar, B. 2011, ICRC (Beijing), 2, 198
Kochanek, C. S. 2016, MNRAS, 461, 371
Koning, A. J., Hilaire, S., & Duijvestijn, M. C. 2005, in AIP Conf. Proc. 769, INTERNATIONAL CONFERENCE ON NUCLEAR DATA FOR SCIENCE AND TECHNOLOGY (Melville, NY: AIP), 1154
Lee, S. 1998, PhRvD, 58, 043004
Linsley, J. 1963, PhRvL, 10, 146
Madau, P., & Dickinson, M. 2014, ARA&A, 52, 415
Mayotte, E. W., Halim, A., Aglietta, P., et al. 2023, ICRC (Nagoya), 444, 365
Muzio, M. S., Unger, M., & Farrar, G. R. 2019, PhRvD, 100, 103008
Muzio, M. S., Unger, M., & Wissel, S. 2023, PhRvD, 107, 103030
Petrucci, C., Halim, A. A., Abreu, P., et al. 2023, ICRC (Nagoya), 444, 1520
Plotko, P., Winter, W., Lunardini, C., & Yuan, C. 2024, arXiv:2410.19047
Protheroe, R. J., & Johnson, P. A. 1996, APh, 4, 253
Puget, J. L., Stecker, F. W., & Bredekamp, J. H. 1976, ApJ, 205, 638
Rodrigues, X., Heinze, J., Palladino, A., van Vliet, A., & Winter, W. 2021, PhRvL, 126, 191101
Saldana-Lopez, A., Domínguez, A., Pérez-González, P. G., et al. 2021, MNRAS, 507, 5144
Tkachenko, O., Abdul Halim, A., Abreu, P., et al. 2023, ICRC (Nagoya), 444, 438
Ueda, Y., Akiyama, M., Hasinger, G., et al. 2014, ApJ, 786, 104
Vietri, M. 1995, ApJ, 453, 883
Watson, A. A. 2022, JHEAp, 33, 14
Waxman, E., & Bahcall, J. N. 1999, PhRvD, 59, 023002
Zhang, B. T., & Murase, K. 2019, PhRvD, 100, 103004